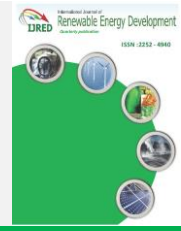




Contents list available at IJRED website

International Journal of Renewable Energy Development

Journal homepage: <https://ijred.undip.ac.id>



Research Article

# Numerical Investigation of Convective Heat Transfer and Fluid Flow Past a Three-Square Cylinders Controlled by a Partition in Channel

Youssef Admi \*, Mohammed Amine Moussaoui, Ahmed Mezrhab

Laboratory of Mechanics & Energy, Faculty of Sciences, Mohammed 1st University, Oujda, Morocco

**Abstract.** This document presents a research article on the control of fluid flow around three heated square cylinders placed side by side in a 2D horizontal channel using a flat plate. The objective of this research is to examine the effect of the position, length and height of a flat plate on fluid flow and heat transfer. For this purpose, numerical simulations are performed by using the Boltzmann double relaxation time multiple network method (DMRT-LBM). The MRT-D2Q9 and MRT-D2Q5 models are used to treat the flow and temperature fields respectively. In contrast to several existing investigations in the literature in this domain which study the passive control of the flow using a horizontal or vertical plate around a single cylinder, this work presents a numerical study on the effect of the position, length and height of a flat plate (horizontal and vertical) on three heated square cylinders on the flow and temperature fields. First, the effect of the position and length of the horizontal flat plate is examined. This study shows that the implementation of a flat plate of length  $L_p = 4D$  at a position  $g=3$  behind the central cylinder reduces the amplitude of the Von Karman Street and allows large and regular heat exchange. Thus, in the second part, the effect of the position and height of the vertical flat plate is studied. The results obtained show that the implementation of a flat plate of height  $h=2D$  at a position  $g=3$  behind the central cylinder improves the thermal exchange between the incoming fluid and the heated cylinders. This numerical work could lead to the prediction of the cooling of the electronic components: The cooling of the obstacles is all the better when the control plate is arranged at  $g = 3$  and its height  $h = 2D$  in the case of the vertical plate or its length  $L_p$  equal to  $4D$  in the case where the plate is implemented horizontally.

**Keywords:** Partition control, Square cylinders, Heat transfer, Flow field, Multiple Relaxation Time Lattice Boltzmann method



@ The author(s). Published by CBIORE. This is an open access article under the CC BY-SA license (<http://creativecommons.org/licenses/by-sa/4.0/>).

Received:31<sup>st</sup> Dec 2021; Revised: 24<sup>th</sup> April 2022; Accepted:10<sup>th</sup> May 2022; Available online: 25<sup>th</sup> May 2022

## 1. Introduction

Due to its intrinsic complexities and importance of the fluid flow and heat transfer and more specifically, the suppression of the vortices shedding around a bluff body has been the subject of several studies in many practical engineering applications, such as flows past an air-plane, a submarine, and an automobile, heat exchanger systems, electronic cooling, gas turbine blades (Florides *et al.*, 2007; Harte *et al.*, 2007; Monat *et al.*, 2018; Shamsoddini *et al.*, 2014). Thus, a host of experimental and numerical investigations has been carried out, during the last years, to understand the flow and heat transfer past of square cylinders, circular or any other geometric shapes of a cylinder in cross flows with or without a control plate (Abbasi *et al.*, 2014; Dey, 2021; Dhiman *et al.*, 2005; Doolan, 2009; Guo *et al.*, 2020; Islam *et al.*, 2015; Koutmos *et al.*, 2004; Kumar *et al.*, 2015; Moussaoui *et al.* 2010; Moussaoui *et al.*, 2010; Rashidi *et al.*, 2015; Rashidi *et al.*, 2016; Sohankar *et al.*, 2018; Turki, 2008; Vamsee *et al.*, 2014). Nevertheless, few works have addressed the

interference effects between multiple cylinders and the number of publications available becomes drastically smaller as the number of cylinders involved increases (Aboueian *et al.*, 2017; Nazeer *et al.*, 2019; Nguyen *et al.*, 2021; Sumner, 2010; Tong *et al.*, 2015). As well, there is very little investigation into the coupling between fluid flow and heat transfer around several cylinders (Admi *et al.*, 2022; Admi *et al.*, 2020; Chatterjee *et al.*, 2012; Moussaoui *et al.*, 2009).

In general, many control methods are categorized into two different categories: passive and active control. Passive control techniques also named vortex suppression equipment, which controls the vortex shedding by modifying the shape of the bluff body or by including additional equipment placed upstream or downstream. This equipment disrupts or prevents the formation of vortex shedding. While, if external energy is provided in the flow field to control vortex shedding, this type of control no longer becomes passive: it is a type of control that has been recently developed, called active control. Noted that the methods of the latter type of control (active

\*Corresponding author:  
Email: [admiyoussef399@gmail.com](mailto:admiyoussef399@gmail.com) (Y. Admi)

control) are more difficult to implement than the passive methods. Adding the plate allows to control or supreme the fluid force acting on a body placed in the channel. This allows for reducing flow-induced structural drag or vibration (Dash *et al.*, 2020; Islam *et al.*, 2015; Kumar *et al.*, 2015; Kumar *et al.*, 2021; Moussaoui *et al.*, 2010; Rabiee *et al.*, 2021; Rashidi *et al.*, 2016; Tamimi *et al.*, 2017; Yang *et al.*, 2020).

The lattice Boltzmann method (LBM) (Mohamad, 2011; Mezrhab *et al.*, 2010; Adeeb *et al.*, 2018; Admi *et al.*, 2022; Admi *et al.*, 2021, 2022; Benhamou *et al.*, 2020, 2022; Breuer *et al.*, 2000; S. Ul Islam *et al.*, 2015; Lahmer, *et al.*, 2022; Lahmer *et al.*, 2022; Lahmer *et al.*, 2019; Moussaoui *et al.*, 2011, 2019, 2021; Rahim *et al.*, 2020; Rashidi *et al.*, 2016) based on multi-relaxation time (DMRT-LBM) is used in numerical simulation because of its intrinsic parallelism of the algorithm, stability compared with the single relaxation time model (BGK) (Bhatnagar *et al.*, 1954; Humières, 2002; Lallemand *et al.*, 2000; McNamara *et al.*, 1988), simplicity of implementation, and ease of incorporating microscopic or mesoscopic interactions. Unlike traditional numerical methods that solve the macroscopic variables such as velocity and density directly, these variables are obtained using the MRT-LBE by moment integrations of the particle distribution function.

The objective of this research is to examine the effect of the position, length and height of a flat plate on the fluid flow and heat transfer around three square cylinders located in a horizontal channel. Firstly, the effect of the position and length of the horizontal flat plate is examined. While in the second study, the effect of the position and height of the vertical flat plate is investigated.

**2. Description of the physical problem Boundary conditions**

*2.1 Statement of the physical problem*

The physical problem studied is shown schematically in Fig. 2 where three identical heated square cylinders (blocks) of width  $D$  are arranged side-by-side vertically in a 2D dimensional horizontal channel and spaced from an equal dimensionless distance  $a$ . An upstream control partition is inserted horizontally and vertically, as illustrated in Fig. 2 a and b. The blockage ratio is fixed to  $\beta = D/H = 1/8$ . In order to reduce the influence of the input and output boundary conditions, the channel length is set to  $L = 24D$ . The heat transfer fluid considered in this study

is air ( $Pr = 0.71$ ) and its physical properties, except the density, are supposed to be constant.

The cylinders are placed at a distance  $X_{in}$  upstream from the inlet section of the channel and  $X_{out}$  downstream from the outlet section of the channel. An infinitely thin partition with different lengths and positions is placed horizontally and vertically behind the central square cylinder. The top and bottom channel walls are assumed to be adiabatic, the airflow incoming with cold temperature which is fixed to  $\theta_c = -0.5$ , each cylinder at a constant hot temperature equal to  $\theta_h = 0.5$ . The flow is fully developed with a parabolic velocity profile at the temperature and velocity gradients are assumed to be zero in the outlet.

*2.2. Boundary conditions*

In the LBM method, the implementation of the boundary conditions occupied a very important place, it's characterized by the simplicity of integrating into the simulation code and plays an important role in the stability and accuracy of the model. In our simulation, for the inlet and outlet of the domain flow, the Zou & He boundary conditions (Zou *et al.*, 1997) are implemented. While the bounce-back boundary conditions are used (Bouzidi *et al.*, 2001) about the solid walls of cylinders and those of the plate.

For the thermal problem, the heat flux boundary conditions are treated by the method originally proposed by Mezrhab *et al.* (Mezrhab *et al.*, 2010). They considered the necessity to move from the macroscopic scale to the mesoscopic scale, which is related to the general term of the distribution function  $g_i$  (Mezrhab *et al.*, 2010):

$$g_j = \sum_{k=0}^4 (M^{-1})_{jk} m_k \quad \text{et} \quad g_1 + g_3 = 2T \left(1 + \frac{a}{4}\right) / 5 \quad (1)$$

Where  $M^{-1}$  is the inverse matrix of the moment and  $a$  is calculated by the preceding formula  $a = \frac{\sqrt{3(4+a)}}{60}$ .

This condition  $g_1 = -g_3 + 2\theta_c \left(1 + \frac{a}{4}\right) / 5$  is applied in the inlet of the channel as well as to the channel input. Whereas for the obstacle limits, we use the same condition, replacing  $\theta_c$  with  $\theta_h$  because the limits of the obstacles are considered hot. Then, adding the condition  $g_2 = -g_4 + 2\theta_c \left(1 + \frac{a}{4}\right) / 5$  for the lower and upper faces of obstacles. Similarly, the adiabatic conditions are used for the canal walls.

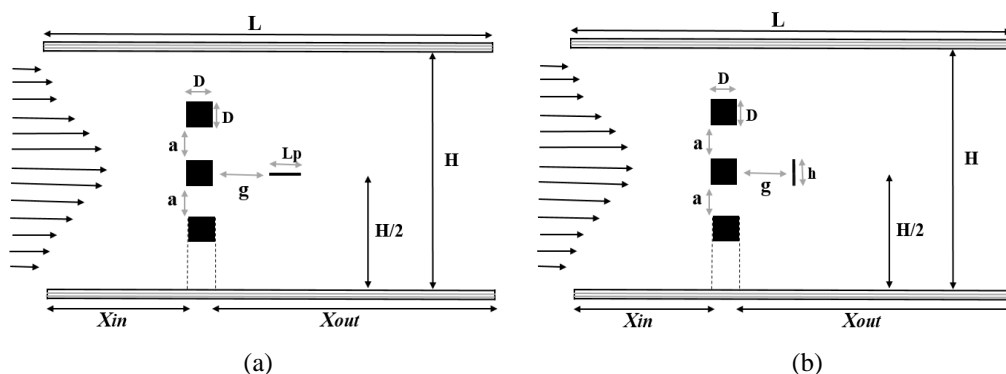


Fig. 1. The physical configuration studied. (a) partition horizontal. (b) partition vertical

### 3. Multi-Relaxation-Time lattice Boltzmann Method

The Multi-relaxation Time Lattice-Boltzmann-Method (LBM-MRT) is a mesoscopic approach that has attracted a lot of attention in the last decades to simulate numerically various problems in many domains: physics, chemistry, biology, medicine etc. This is due to its major advantages such as its high precision, its simplicity, efficiency, and flexibility for most physical problem fluid flow and heat transfer in different geometries, and also, the reduced computational time compared to classical CFD methods. Because of its convergence and compatibility, the MRT-D2Q9 model and the MRT-D2Q5 model are chosen to treat the flow and the temperature fields respectively(A. A. Mohamad, 2011).

In general, the Boltzmann transport equation for a system without external forces can be written as:

$$\frac{\partial f}{\partial t} + c \frac{\partial f}{\partial r} = \Omega(f) \tag{2}$$

where  $\Omega$  is the collision operator developed by D’Humières (Humières, 2002) using the LBM-BGK model.

This equation consists of two parts: the left part represents the advection (propagation) step while the right part represents the collision step. In general, at time  $t$ , the state of the system is known. That is, at each node, the value of  $f_i$  is known. We seek to know the state of the system at the next time  $t + \Delta t$ . For this purpose, a space-time discretization of the function  $f_i$  which represents the density distribution of the particles is necessary. Equation 2 illustrates the discretized Boltzmann equation:

$$f_i(x + e_i, t + \Delta t) - f_i(x, t) = \Omega_i(f) \quad i = 0, \dots, 8 \tag{3}$$

During the propagation phase, each particle moves towards the adjacent node following its velocity direction. Only one particle is allowed per node, therefore, when several particles arrive at the same location, the collision phase determines their interactions and how they change position. The particles thus move synchronously on a regular network by satisfying several assumptions:

Introducing the evolution proposed by D’Humières the previous expression will be written as follows (Humières, 2002).

$$f_i(x + e_i, t + 1) - f_i(x, t) = M_f^{-1} \times S_f [m_f(x, t) - m_f^{eq}(x, t)] \quad i = 0, \dots, 8 \tag{4}$$

With  $m$  and  $m^{eq}$  are the moment’s vector, and the equilibrium momentum, respectively:

$$m = (m_0, m_1, m_2, m_n)^T; \quad m^{eq} = (\rho, e^{eq}, \varepsilon^{eq}, j_x, q_x, j_y, q_y, p_{xx}, p_{xy})^T \tag{5}$$

The choice of the equilibrium functions  $m_i^{eq}$  will determine the equivalent macroscopic equations.

$$\begin{aligned} m_0^{eq} &= \rho \\ m_1^{eq} &= j_x \\ m_2^{eq} &= j_y \\ m_3^{eq} &= -2\rho + 3(j_x^2 + j_y^2) \\ m_4^{eq} &= \rho - 3(j_x^2 + j_y^2) \end{aligned} \tag{6}$$

$$\begin{aligned} m_5^{eq} &= -j_x \\ m_6^{eq} &= -j_y \\ m_7^{eq} &= (j_x^2 - j_y^2) \\ m_8^{eq} &= j_x j_y \end{aligned}$$

Where

$$\begin{aligned} j_x &= \rho u_x = \sum_i f_i^{eq} c_{ix} \\ j_y &= \rho u_y = \sum_i f_i^{eq} c_{iy}. \end{aligned} \tag{7}$$

The transformation Matrix  $M$  denotes the correspondence between the velocity and moment spaces. where:  $m = Mf$  and  $f = M^{-1}m$ . The matrix  $M$  of order 9 is given by (A. A. Mohamad, 2011):

$$M = \begin{pmatrix} 1 & 1 & 1 & 1 & 1 & 1 & 1 & 1 & 1 \\ 0 & 1 & 0 & -1 & 0 & 1 & -1 & -1 & 1 \\ 0 & 0 & 1 & 0 & -1 & 1 & 1 & -1 & -1 \\ -4 & -1 & -1 & -1 & -1 & 2 & 2 & 2 & 2 \\ 4 & -2 & -2 & -2 & -2 & 1 & 1 & 1 & 1 \\ 0 & -2 & 0 & 2 & 0 & 1 & -1 & -1 & 1 \\ 0 & 0 & -2 & 0 & 2 & 1 & 1 & -1 & -1 \\ 0 & 1 & -1 & 1 & -1 & 0 & 0 & 0 & 0 \\ 0 & 0 & 0 & 0 & 0 & 1 & -1 & 1 & -1 \end{pmatrix} \tag{8}$$

Likewise, the MRT-LBM is implemented to compute the advection-diffusion equation of temperature, using the second function of distributions  $g_i$ . For the reason of simplicity and compatibility, it is recommended to use the D2Q5 model (Fig.2). In this model (D2Q5) the evolution of the fluid particles from one node of the grid to an adjacent node with discrete velocities is given by:

$$g_i(x + c_i \Delta t, t + \Delta t) = g_i(x, t), \quad i = 1, 2, 3, 4 \tag{9}$$

For thermal boundary conditions, the following expressions (8) are used to convert them from the macroscopic scale to the mesoscopic level in distribution function(A. Mezrhab, M. A. Moussaoui, M. Jami, H. Naji, M. H. Bouzidi, 2010):

$$g_j = \sum_{k=0}^4 (M^{-1})_{jk} m_k \quad et \quad g_1 + g_3 = \frac{2T(1+\alpha)}{5} \tag{10}$$

Where  $M^{-1}$  is the inverse matrix of the moment and  $\alpha$  is calculated by the preceding formula  $\alpha = \frac{\sqrt{3(4+\alpha)}}{60}$ . For the thermal problem, the distribution functions  $g_i$  are expressed:

$$g_i(x + e_i, t + 1) - g_i(x, t) = \Omega_i(g) \quad i = 0, \dots, 8 \tag{11}$$

The collision step could be presented by the MRT-TLBM model:

$$g_i(x + e_i, t + 1) - g_i(x, t) = M_g^{-1} \times S_g [m_g(x, t) - m_g^{eq}(x, t)] \quad i = 0, \dots, 8 \tag{12}$$

$M^{-1}$  designates the inverse of the transformation matrix for the D2Q5 model in which the matrix  $M$  is of order 5. This matrix  $M$  is given by (A. A. Mohamad, 2011) :

$$M = \begin{pmatrix} 1 & 1 & 1 & 1 & 1 \\ 0 & 1 & 0 & -1 & 0 \\ 0 & 0 & 1 & 0 & -1 \\ -4 & 1 & 1 & 1 & 1 \\ 0 & 1 & -1 & 1 & -1 \end{pmatrix} \tag{13}$$

However, for the D2Q5 model, the dimensionless temperature  $\theta$  is the only conserved quantity and is obtained by:

$$\theta = \sum_{i=0}^N g_i \tag{14}$$

#### 4. Validation of the simulation code

The present code is validated with the work obtained by Breuer *et al.* (Breuer *et al.*, 2000). They realized numerical research using the finite volume method and

LBM method to simulate the flow past a single square cylinder for different values of the Reynolds number ( $Re = 5 - 200$ ). Figure 3 shows the velocity components along the centerline for a Reynolds number equal to 100. The comparison of these components is an excellent agreement between our results and the results presented by Breuer *et al.* (Breuer *et al.*, 2000).

We have already carried out a study of laminar flow and heat transfer in a horizontal channel containing three heated obstacles (Fig. 4) (Youssef Admi *et al.*, 2019) but without a control device. Figure (4) presents the streamlines and isotherms for  $Re = 100$ .

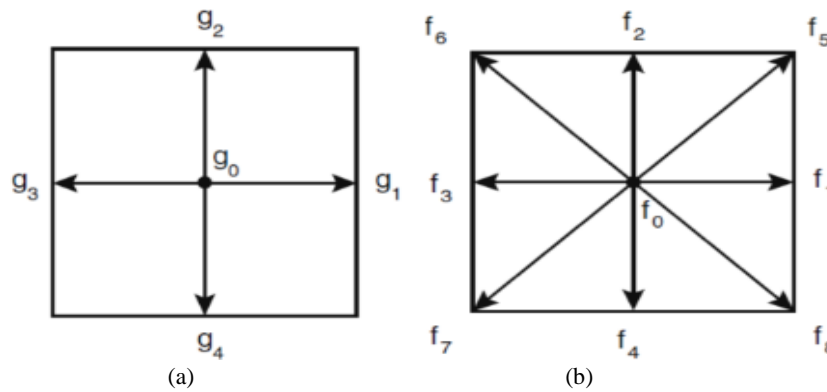


Fig. 2. (a) The two-dimensional D2Q9 velocity. (b) The D2Q5 for thermal problem.

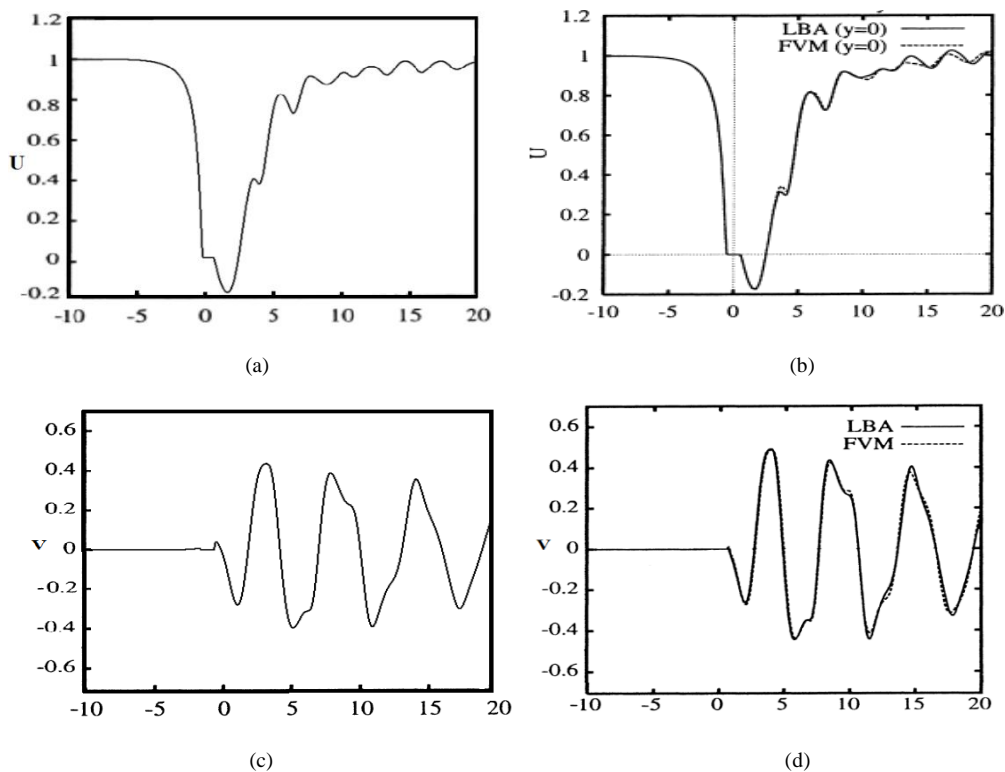


Fig. 3. Velocity profiles along the centerline at  $Re = 100$ : (a) and (c) Present work, (b) and (d): (Breuer *et al.*, 2000)

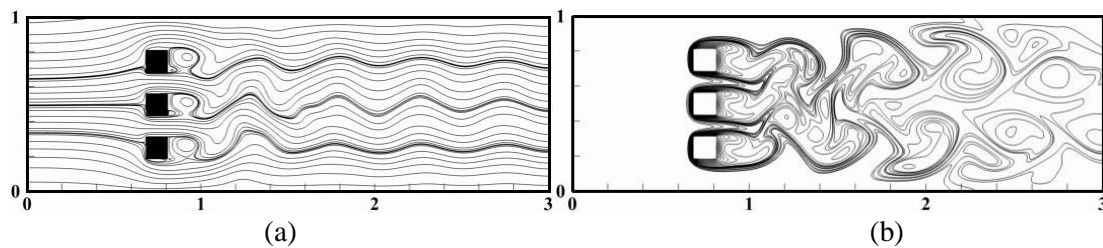


Fig. 4. Streamlines (a) and isotherms (b) for the case without partition

## 5. Result and Discussion

In the literature, several investigations have been performed with study the flow of a fluid coupled to heat transfer around an obstacle. However, a small number of studies have been carried out around several obstacles compared to those carried out around a single obstacle.

In this paper, numerical calculations were realized for a fluid flow around three side-by-side square cylinders equally spaced and controlled by a horizontal and vertical partition respectively. These investigations are performed at fixed Reynolds number  $Re = 100$ . This number is based on the cylinder diameter  $D$  and the maximum flow velocity  $U_{max}$  of the parabolic inlet profile. For the two states of the partition (horizontal or vertical), the effect of the location of the partition behind the central block is firstly studied by fixing its length ( $L_p = D$ ). Then, the effect of the length of the partition is examined while fixing its position.

### 5.1. Effects of horizontal partition location

As mentioned earlier, several studies exist in the literature that treats the flow of fluids around one or more obstacles (Ali *et al.*, 2012; Chatterjee *et al.*, 2013; Dey, 2021; Dhiman *et al.*, 2005; Guo *et al.*, 2020; Han *et al.*, 2013; Islam *et al.*, 2016; Kumar *et al.*, 2015; Malekzadeh *et al.*, 2012; Manzoor *et al.*, 2020; Rashidi *et al.*, 2015; Sohankar *et al.*, 2018; Wu *et al.*, 2006; Zhou *et al.*, 2005). Han *et al.* (Han *et al.*, 2013) used the finite element scheme (CBS) to study the flow around two square cylinders arranged horizontally side by side at a fixed Reynolds number. The study of the effect of the spacing between the two cylinders shows the existence of three flow models. Likewise, Islam *et al.* (Islam *et al.*, 2016) performed a numerical study to analyze the effect of low Reynolds number "Re" and spacing "g" on the flow around three-square cylinders aligned in line without implementing any control instrument. These authors used the MRT-LBM and observed seven different flow patterns for different values of "Re" and "g".

In the first part of this investigation, the effect of the gap spacing between the central block and partition has been studied. To this end, four cases ( $0 \leq g \leq 3$ ) are treated of which the dimensionless length of the partition remains fixed ( $L_p/D = 1$ ).

Figures 5a-d show an asymmetric distribution (with regard to the central axis of the channel) of streamlines around the three cylinders. A recirculation and a stagnation zone are clearly visualized in all cases behind

the block at the top and the block at the bottom, whereas two recirculations are observed behind the central block. These two recirculations are either located on the upper and lower sides of the partition as shown in figures 5.a-c, or they appear to belong to the gap between the block and the partition. Then, they interact with the shear layers of the upper and lower blocks and form a large circulation behind the control partition except in the last case where there is a small area of stagnation on the trailing edge of the partition. This large recirculation will disturb the flow along the channel. The amplitude of this recirculation decreases with increasing separation distance and the flow pattern is characterized by the alternate shedding vortices behind the control plate. This phenomenon is well known as the von Karman vortex streets.

Note that for very small values of  $Re$  (not shown here), a creeping flow is obtained for each obstacle, and the flow around an obstacle is not affected either by the presence of nearby obstacles or by the presence of the control partition. Cancellation of this symmetry is observed while increasing the Reynolds number.

The coupling between fluid flow and heat transfer around multiple cylinders is poorly studied in the literature (Admi *et al.*, 2022; Admi *et al.*, 2022; Chatterjee *et al.*, 2013; Lahmer *et al.*, 2022; Moussaoui *et al.*, 2021; Wu *et al.*, 2006). Chatterjee *et al.* (Chatterjee *et al.*, 2013) present a 2D numerical study of fluid flow and heat transfer by mixed convection around two heated square cylinders placed in tandem for Reynolds number range  $50 \leq Re \leq 150$ . The relationship between the spacing and the size of the cylinders  $S/d$  is studied. Also, the effect of superimposed thermal thrust on the flow and isothermal patterns is presented and discussed. Global flow and heat transfer quantities such as global drag and lift coefficients, local and area-averaged Nusselt numbers, and Strouhal numbers are calculated and discussed for different Reynolds and Richardson numbers and spacing ratios. The notable contribution is the quantification of the critical spacing ratio, which is observed to decrease with the increasing thermal buoyancy effect for a specific Reynolds number. Also, Wu *et al.* (Wu *et al.*, 2006) use a semi-implicit finite element method to study the effect of the interaction of the transient mixed convective flow between the circular cylinders and the channel walls on the heat transfer. They found that the isotherms are affected by different space/diameter ratios "S", Reynolds numbers "Re". Also, they observed that maximum heat transfer exists between the three circular cylinders and the channel walls in the case where  $S=0.75$ .

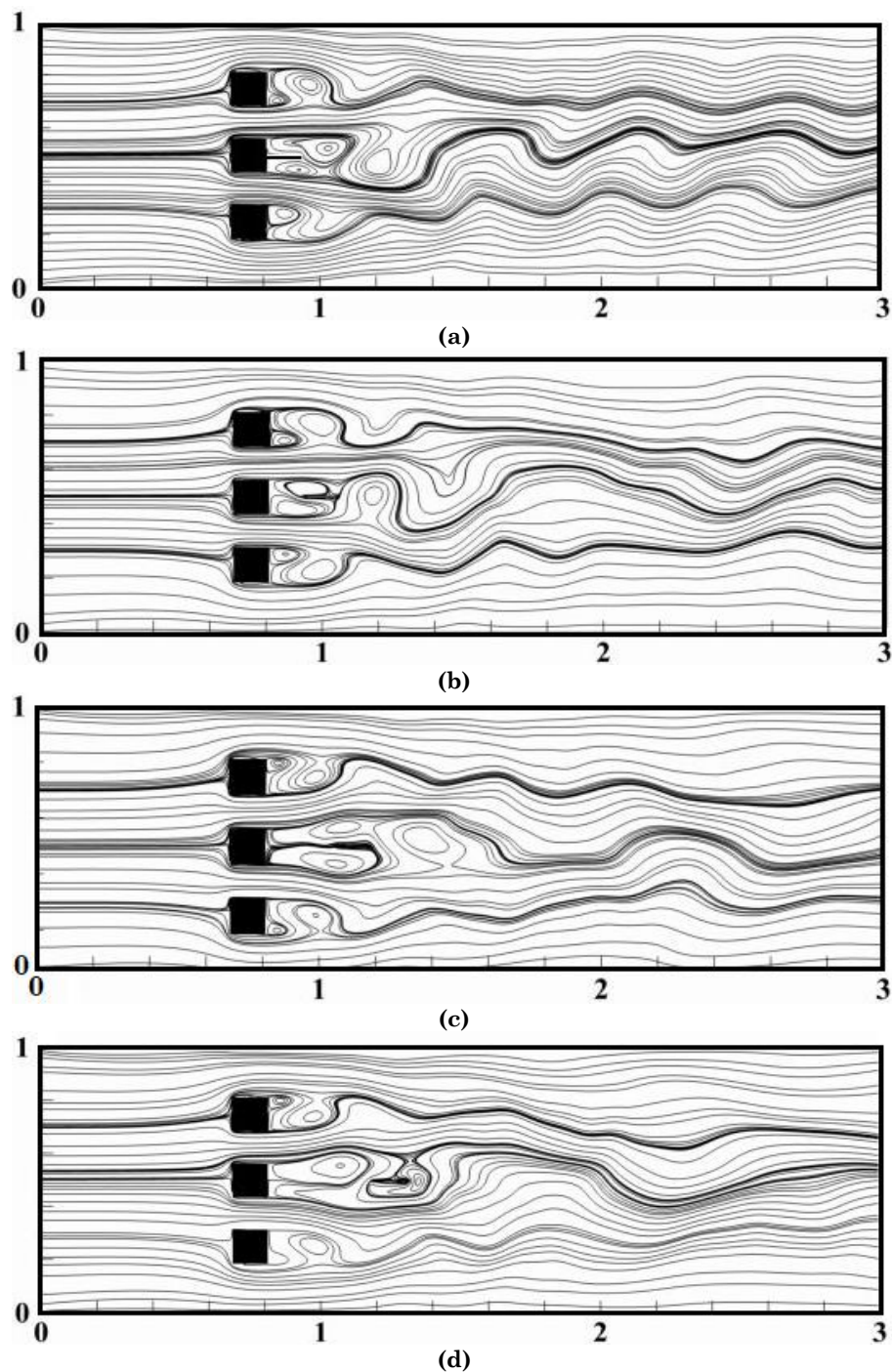


**Fig. 5.** Streamlines for different horizontal partition positions at  $L_p/D=1$  and  $Re = 100$ : (a)  $g = 0$ ; (b)  $g = 1$ ; (c)  $g = 2$ ; (d)  $g = 3$ .

Fig. 6 shows the isotherms around the three cylinders for  $Re = 100$  and for spacing gaps varying from  $g = 0$  to  $g = 3$ , the isothermal contours are more strongly affected downstream than upstream by the presence of obstacles. In addition, the presence of the partition has also an influence on the isothermal lines, while forming a jet flow along the channel. Downstream of the cylinder, the wake becomes narrower and depends on the position of the partition. In the case where the partition is attached to the central obstacle (fig. 6a) or if there is no control partition (fig. 4), a significant formation of vortices and a large wake is observed. This flow can be locally accelerated to improve heat transfer. An intense temperature gradient forms

around the obstacles, indicating the existence of important heat exchange in these regions. However, when increasing the distance between the central cylinder and the control partition, the number of vortices formed decreases and the wake becomes narrower but remains unstable and asymmetrical.

Note that in all cases, a large temperature gradient is visible from the contours, particularly near the front face, which has thinner thermal boundary layers around which the highest heat transfer rates occur near this face. The transport of thermal energy is performed by the flow in the wake

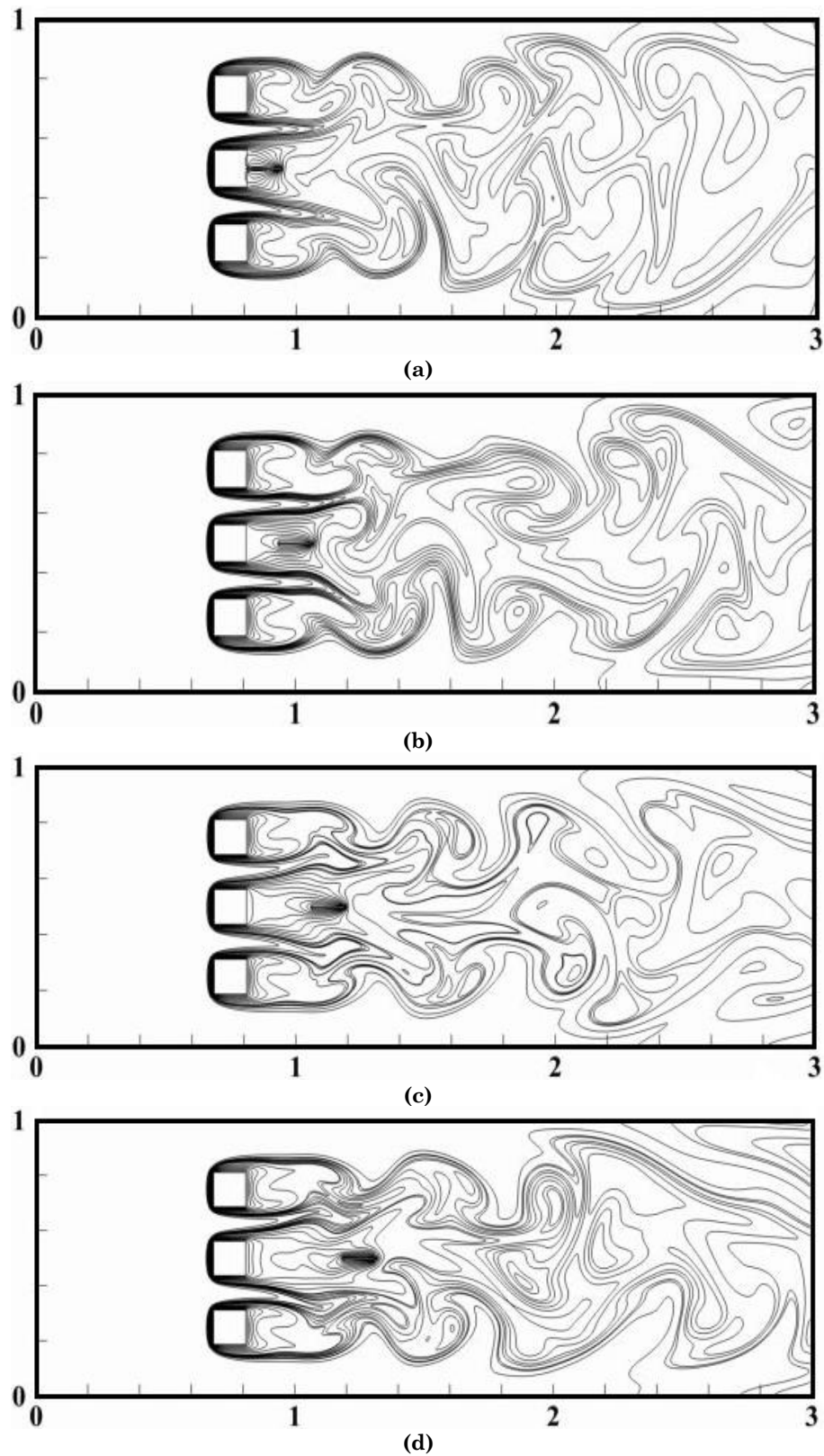


**Fig. 6.** Isotherms for different horizontal partition positions at  $L_p/D = 1$  and  $Re = 100$ : (a)  $g = 0$ ; (b)  $g = 1$ ; (c)  $g = 2$ ; (d)  $g = 3$ .

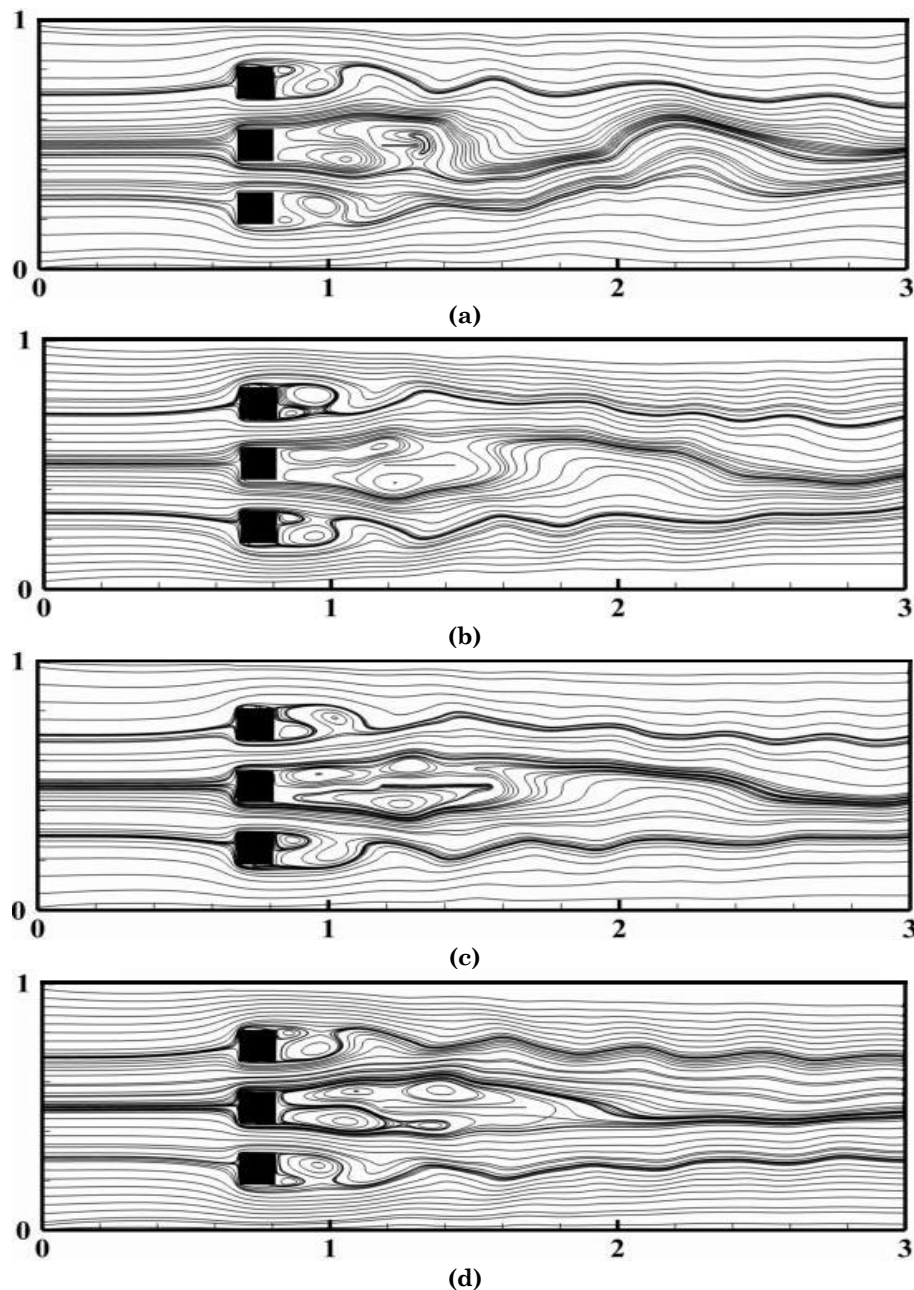


**Fig. 7.** Streamlines for different partition length at  $g=3$  and  $Re = 100$ : (a)  $L_p = 1D$ ; (b)  $L_p = 2D$ ; (c)  $L_p = 3D$ ; (d)  $L_p = 4D$

### 5.2. Effects of horizontal partition length

Very limited research has been conducted on flow control coupled with heat transfer around multiple cylinders. While there are numerical and experimental investigations (Ali *et al.*, 2012; Manzoor *et al.*, 2020; Turki, 2008) that study flow control with or without coupling to heat transfer around a single cylinder using simple control instruments (passive control). Turki *et al.* (Turki, 2008) using a splitter plate for passive control of vortex shedding behind a square cylinder in laminar flow. Numerical calculations were performed at different Reynolds numbers  $110 \leq Re \leq 200$  and for a blocking ratio  $\beta = h/H = 1/4$ . They investigated the effect of the length of the splitter plate and its location in the wake region on the instantaneous flow fields. They found that the disappearance of vortex shedding corresponds to a critical length of the splitter plate  $L_c = 2.2$ .

Likewise, numerical simulations were conducted by Manzoor *et al.* (Manzoor *et al.*, 2020) to examine the effect of control rod size ( $4 \leq d_1 \leq 20$ ) and spacing ratio ( $1 \leq g \leq 5$ ) on the flow around a square cylinder at a fixed Reynolds number ( $Re = 160$ ) using the lattice Boltzmann method (LBM). They found that vortex shedding is completely suppressed at  $(g, d_1) = (1, 12)$ ,  $(2, 12)$ , and  $(2, 16)$  where the stable flow mode exists. In addition, they found that at a large spacing, where  $g = 5$ , the effect of the control rods on the main cylinder disappears.

In the second investigation, the effect of the partition length has been studied by fixing the gap spacing between the central block and the control partition at  $g = 3$  for  $Re = 100$ . Four cases are realized in this study whose length of the partition  $L_p$  is varied from  $1D$  to  $4D$ .

Fig. 6 shows the instantaneous streamlines visualization plots in which a recirculation in the space between the central cylinder and the control plate is

observed in all cases studied, the size of this recirculation increases with the increasing distance between the obstacle and the control partition. The shear layers delivered by the ends of the obstacles form recirculation on the upper and lower faces of the control plate. These recirculation either produce undulations along the channel and produce Von Karman vortices (fig. 6a-b) or they are partially or totally peeled off and amortized along with the faces of the plate as shown in fig. 6 c-d.

Two flow models are obtained. A flow model in which a strong vortex shedding is induced, as shown in Fig. 6(a-b). In this pattern, a big vortex, in the formation region, is distended and interacted significantly along the horizontal axis, resulting in a large formation region in terms of shed vortices just behind the control partition. These shed vortices are stronger because of the small length

of the control partition. In the second model, the flow is characterized by a slightly undulating wake. The big vortex formed in the region spacing the middle cylinder and the control partitions distended and interacted with the vortex formed around the control plate. Thanks to the increase in the length of the partition, these interactions are damped along the upper and lower surface of this control partition. Consequently, an almost complete suppression of the vortices was observed in the last case studied. In this case, the flow regime becomes almost stable and symmetrical.

In this investigation, the effect of the partition length has been studied. For this reason, four cases ( $L_p=1D-4D$ ) are treated where the gap spacing between the central block and partition is fixed at  $g = 3$ .

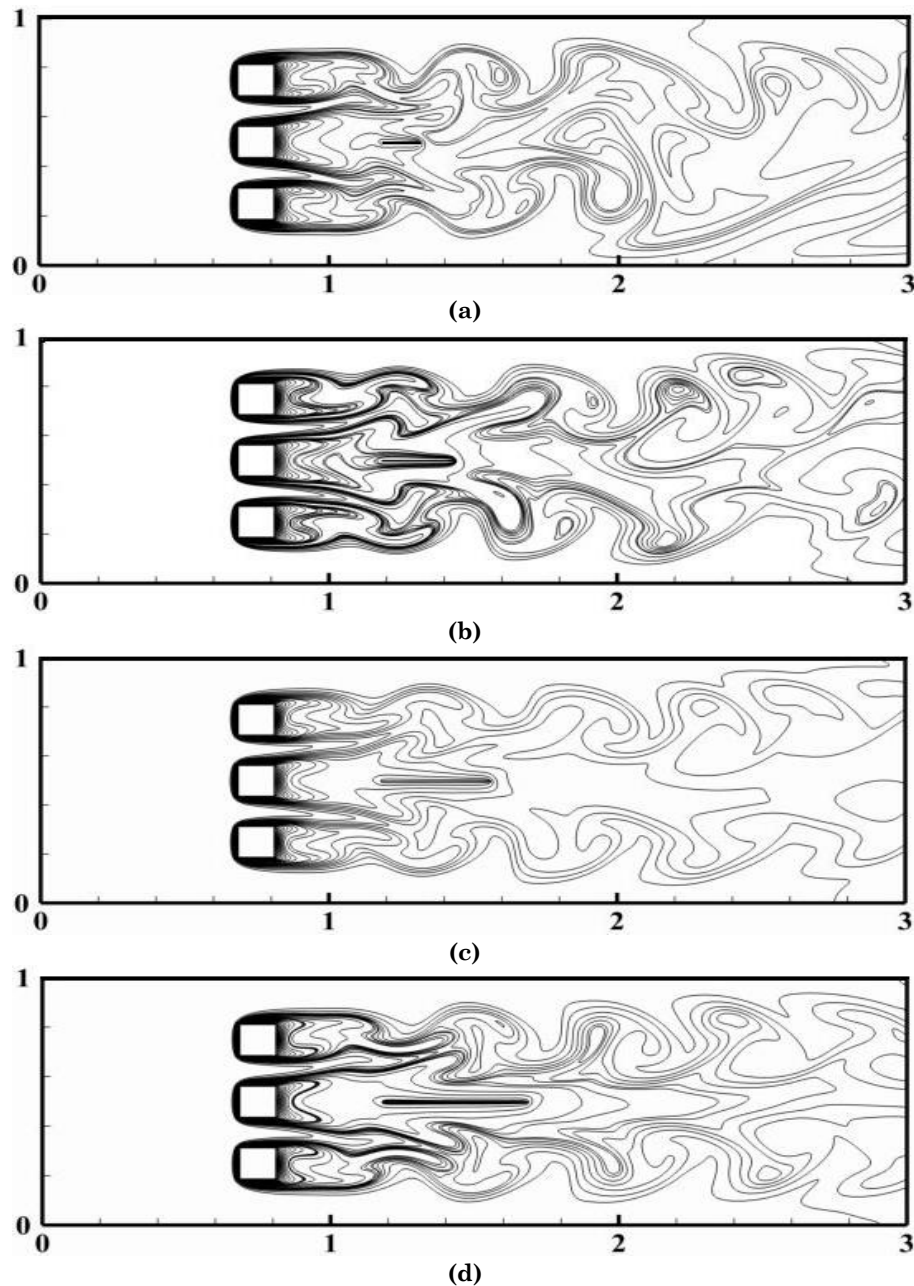


**Fig. 8.** Isotherms for different partition lengths at  $g = 3$  and  $Re = 100$ : (a)  $L_p = 1D$ ; (b)  $L_p = 2D$ ; (c)  $L_p = 3D$ ; (d)  $L_p = 4D$

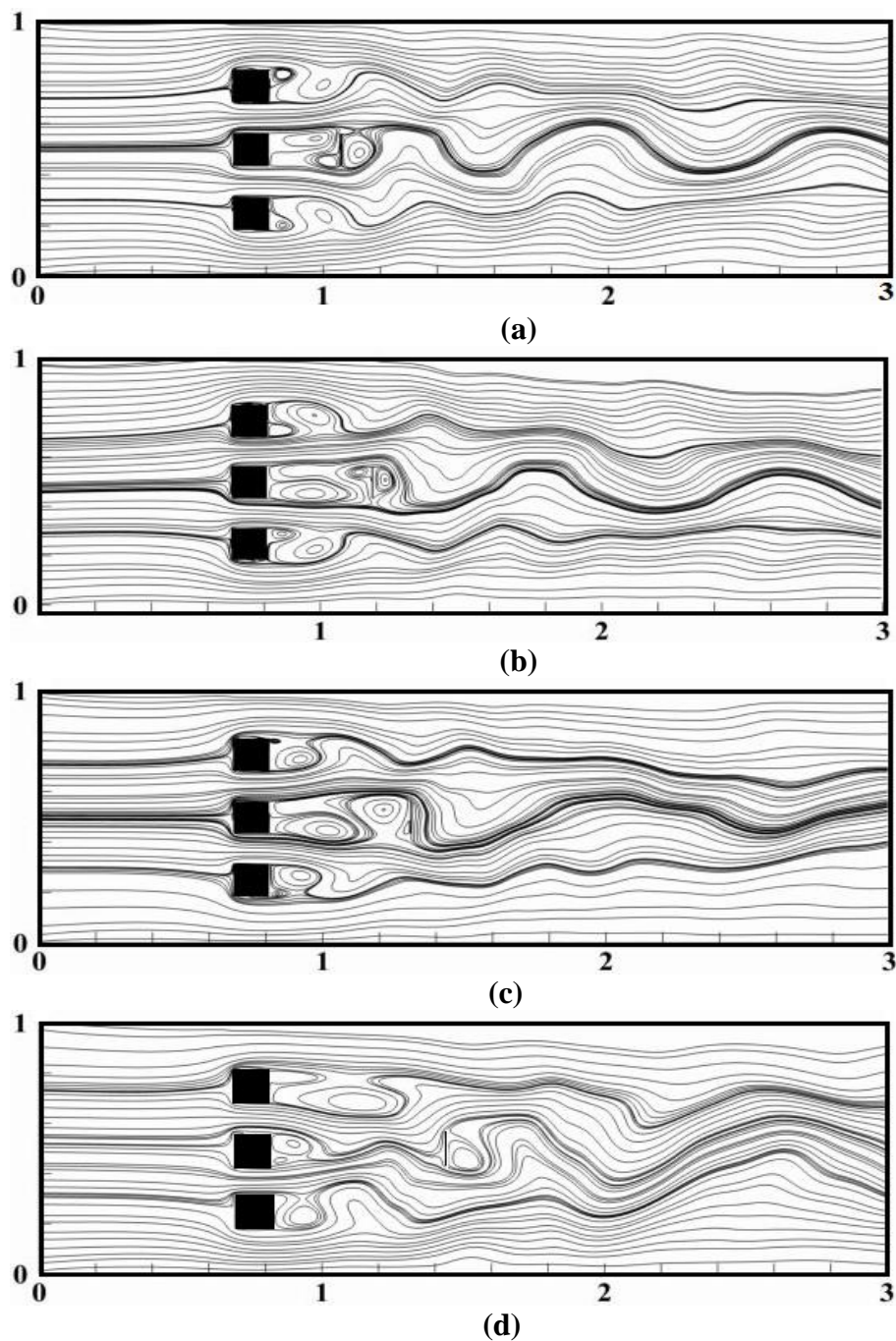


**Fig. 9.** Streamlines for different vertical partition positions at  $h = D$  and  $Re = 100$ : (a)  $g=2$ ; (b)  $g = 3$ ; (c)  $g = 4$ ; (d)  $g = 5$

Fig. 8 shows the isotherms contours of the flow controlled by a plate positioned at  $g=3$  with various lengths. Likewise, the isothermal contours are affected by the presence of obstacles and by the presence of the partition. This influence is observed by the formation of a jet flow along the channel. When  $L_p = 1D-2D$  (Figs. 8a-b), alternate vortex shedding behind the square cylinder is observed. The width of the Karman vortex street becomes gradually narrower as the control plate length increases. An intense temperature gradient forms around the obstacles, indicating the existence of important heat exchange in these regions. However, when  $L_p = 3D-4D$  (Fig. 8 c-d), the vortex shedding becomes weak and the flow becomes quasi-stable and symmetrical in the last case. This indicates that the vortex shedding behind the square cylinders is effective and can be annulled or its amplitude

decreases if the control plate is placed at a suitable position with the proper length. It can be seen that the isotherms are elongated in the direction of flow and the regime becomes quasi-stable and symmetrical with respect to the channel axis and show a thermal boundary layer close to the walls of the three obstacles. A temperature gradient induced more in the rear face of the obstacles is visible from the contours, especially in the last case

### 5.3. Effects of vertical partition location

In this section, the control flat plate is arranged vertically behind the square obstacles. Indeed, the effect of the position and length of the control flat plate on streamlines and isotherms is investigated at fixed

Reynolds number  $Re = 100$ . In each study, four cases are presented.

Fig. 9 presents the streamlines for spacing gaps ranging from  $g = 2$  to  $g = 5$ . This figure shows that the size of the recirculation behind the central obstacle increases with increasing spacing up to  $g = 4D$ , whereas after this spacing ( $g \geq 4$ ) the size of the recirculation decreases, while the size of the recirculation behind the top and bottom obstacle increases. Indeed, the shear layers delivered by the extremity of the central block have enough space by forming a recirculation behind the central block. This provokes undulations in the gap space between the central obstacle and the control plate. These undulations, of large amplitudes, disturb the flow downstream of the partition and result in an unstable and asymmetric regime. In Figure 9a-c, a recirculation formed behind the control plate interacts with the shear layers delivered by the extremity obstacles and results in an almost symmetrical and weakly perturbed Von Karman Street flow compared to the cases where  $g \geq 4$ .

Figure 10 shows the visualization of the isotherm contours around the three heated square obstacles followed by a flat plate. In this isotherm contour, the vortex shedding tends to dissipate more rapidly and intensely behind the obstacles, especially in the case where the position of the plate  $3 < g \leq 5$ . Indeed, for this gap, the layers delivered by the top and bottom edge of the obstacle strike the control plate and consequently form small vortices in the intermediate zone allowing a strong heat exchange in these cases. Whereas in the closest case where  $2 \leq g \leq 3$ , a large part of the shear layers dip behind the partition (the central obstacle and the partition are considered as one body), resulting in weak heat exchange. Likewise, in the case of  $g = 4$ , the totality of the shear layers plunges into the intermediate space by encountering the control plate, which strongly disturbs the flow in the intermediate zone. This increases the heat exchange between the fluid and the blocks, especially with the backs of the blocks.

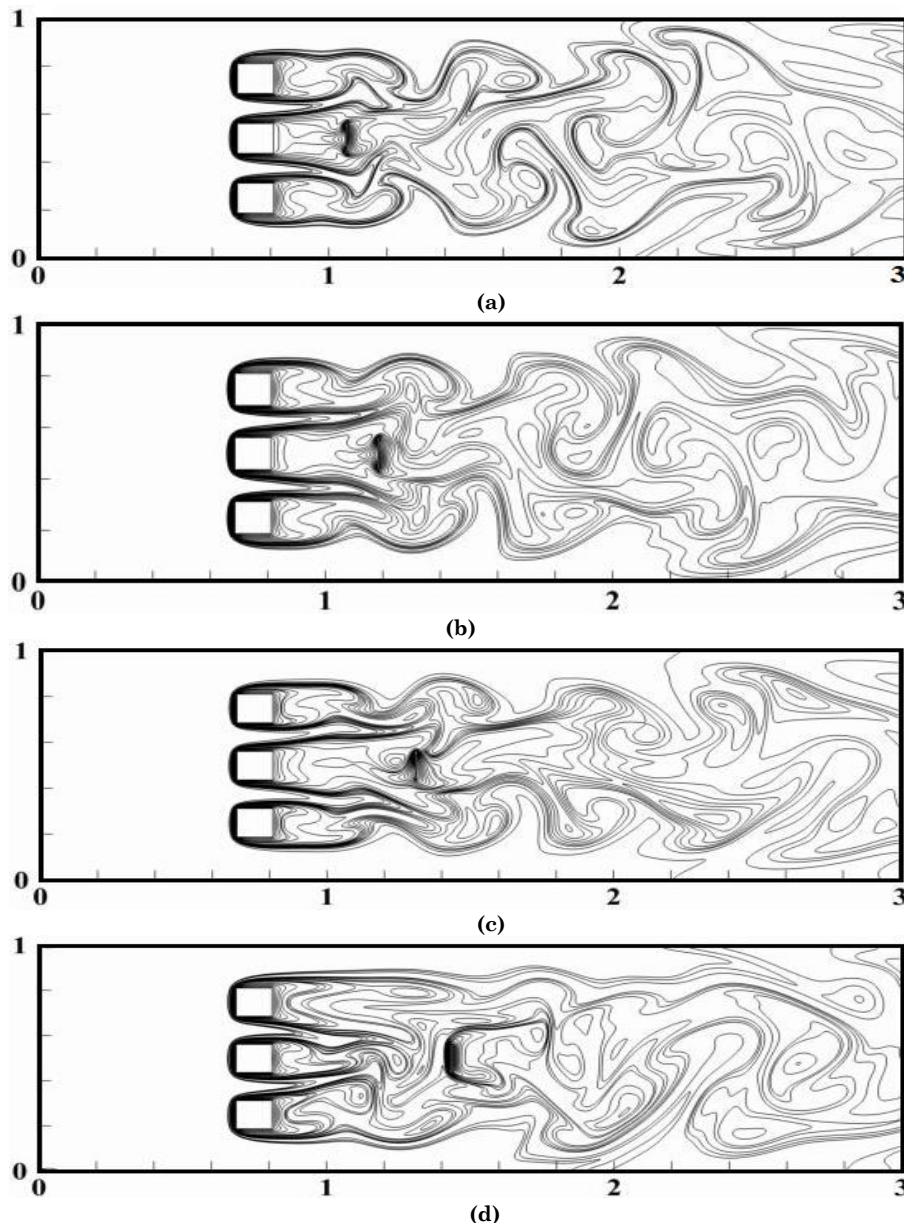


Fig. 10. Isotherms for different partition positions at  $h = D$  and  $Re = 100$ : (a)  $g = 2$ ; (b)  $g = 3$ ; (c)  $g = 4$ ; (d)  $g = 5$ .

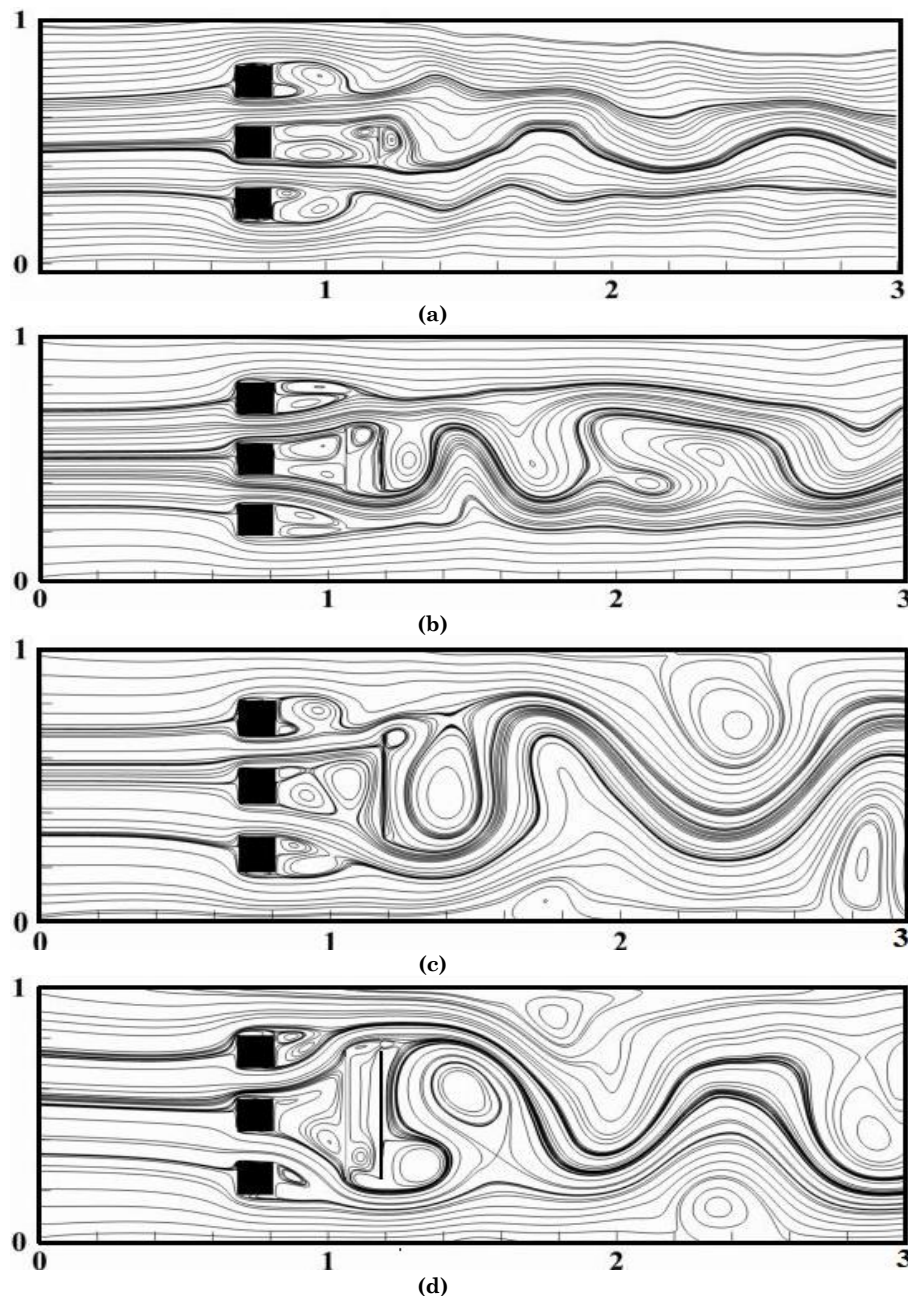
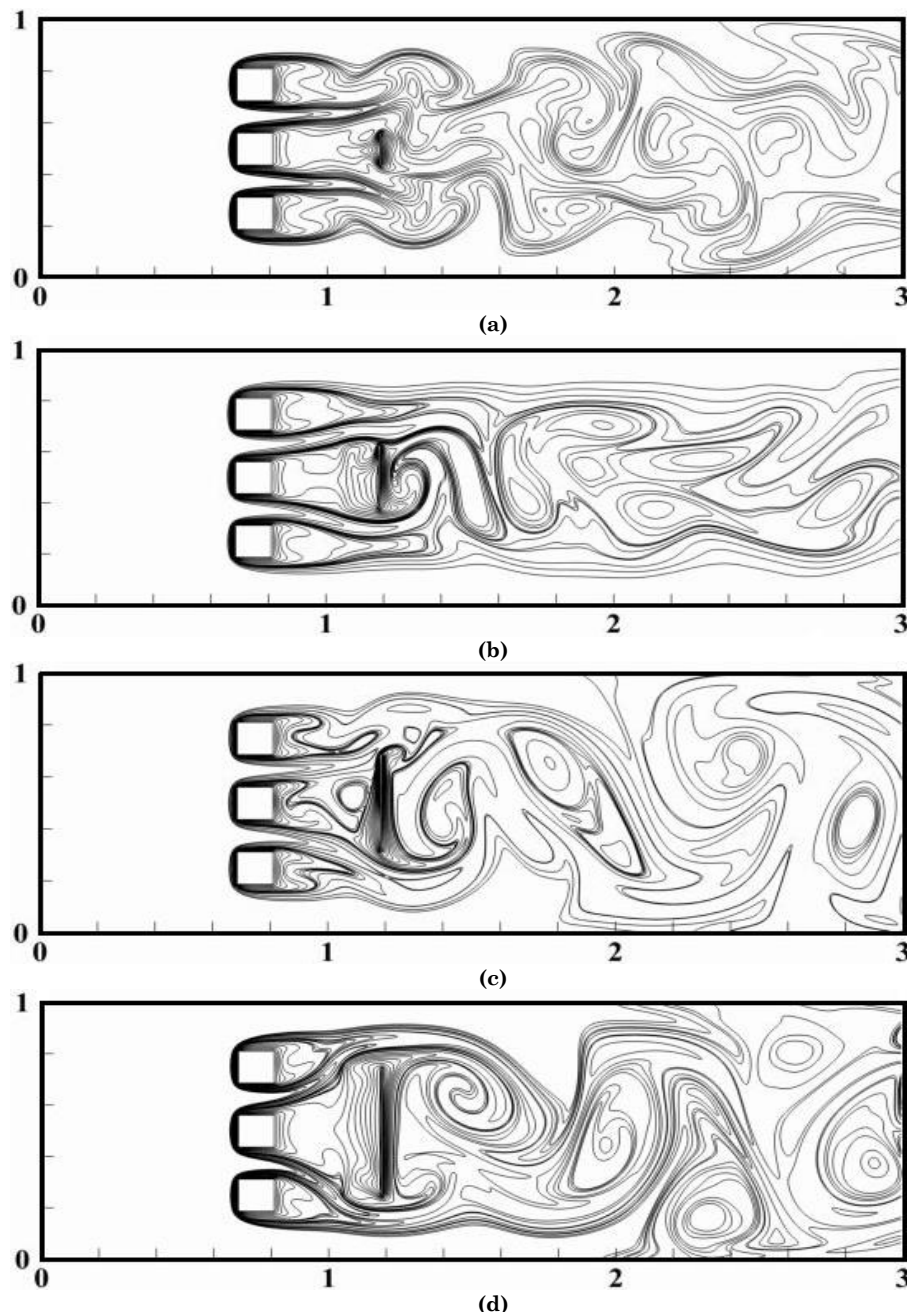


Fig. 11. Streamlines for different partition heights at  $g = 3$  and  $Re = 100$ : (a)  $h = 1D$ ; (b)  $h = 2D$ ; (c)  $h = 3D$ ; (d)  $h = 4D$

#### 5.4. Effects of vertical partition length

The purpose of this last investigation is to study the influence of the height of the plate on the flow and the heat transfer. Indeed, in the literature, there are investigations that study the effect of the height of the control plates on the flow field and isotherms around a square cylinder. Malekzadeh *et al.* (Malekzadeh *et al.*, 2012) perform a numerical study to examine the effect of the position "g" and width "S" of the control plate on laminar flow coupled with heat transfer around a square cylinder. The results of this study show that the optimal position and width for the control plate are a distance of  $3W$  from the cylinder and width of  $0.5W$ , respectively, where almost maximum

reduction in fluid forces and minimum reduction in heat transfer are provided. Similarly, Zhou *et al.* (Zhou *et al.*, 2005) use a flat control plate to control the flow around the square cylinder in a two-dimensional channel at a fixed Reynolds number  $Re = 250$ . The effects of the control plate height on the streamlines and on the fluid forces acting on the square cylinder have been studied. This study shows that there is a significant reduction in these fluid forces. while in this article, Figures 11 and 12 illustrate respectively the streamlines and the isotherms for various heights  $1D \leq h \leq 4D$  at  $Re = 100$ . From these figures, one can note that, in all cases, the presence of plate after the square obstacles induce unstable vortices, which promote heat transfer.



**Fig. 12.** Isotherms for different partition heights at  $g = 3$  and  $Re = 100$ : (a)  $h = 1D$ ; (b)  $h = 2D$ ; (c)  $h = 3D$ ; (d)  $h = 4D$

For the first case where the length of the plate  $h = 1D$  (Fig.12a and Fig.13a), we observe that there is a recirculation followed by a stagnation behind the top and bottom obstacles. While there are two recirculations behind the central obstacle, these recirculations interact with the part of the thermal layers issued from the obstacle's extremity and which has confronted the control plate, thus allowing a rather weak thermal exchange. On contrary, when  $h = 2D$ , two recirculations are observed behind each obstacle. Similarly, the thermal layers behind the top and bottom obstacle have the same size and the wakes oscillate in-phase mode. A large temperature gradient is observed behind each obstacle, which means that there is a large heat exchange between the fluid and the heated obstacles. Note that the general behavior of the flow fields and isotherms appear regular and symmetrical around obstacles.

For  $h = 3D-4D$  (Fig.12c-d, Fig.13c-d), An alternating Karman Vortex Street is observed in the wake region downstream of the control partition. These structures are certainly due to the strong jet interaction between the obstacles and control partition. Intense temperature gradients are formed between the obstacles and the control plate indicating the existence of significant fluidic forces exerted on the obstacles. While the large recirculation is seen in the case where  $h = 4D$ , which indicates that the fluid is locked in the intermediate area. This can weaken the rate of heat exchange.

## 6. Conclusions

The present work presents the results of a numerical investigation on the control of fluid flow around three heated square cylinders situated side by side in a 2D

horizontal channel using a flat plate at a fixed Reynolds number of 100 by using the MRT-LBM. The developed code has been validated with previous work and the results obtained show a good agreement with those available in the literature. The study of the effect of the gap spacing  $g$ , the length  $L_p$  and the height  $h$  of the control plate implemented horizontally or vertically is presented in the form of the streamlines and isotherms around these three obstacle squares. First, the effect of the position and length of the horizontal flat plate is examined. This study shows that the implementation of a flat plate significantly increases the thermal exchange between the fluid and the rear face of the cylinders. Likewise, the results obtained show that the use of a horizontal flat plate of length  $L_p = 4D$  at a position  $g=3$  behind the central cylinder reduces the amplitude of the Von Karman Street and allows significant and regular heat exchange. Thus, in the second part, the effect of the position and height of the vertical flat plate is studied. The results obtained show that the implementation of a vertical flat plate disturbs the flow along the channel. Also, the results show that the use of a flat plate of height  $h=2D$  at a position  $g=3$  behind the central cylinder improves the heat exchange between the incoming fluid and the heated cylinders. This numerical work could lead to the prediction of the cooling of the electronic components: The cooling of the obstacles is all the better when the control plate is placed at  $g = 3$  and its height  $h = 2D$  in the case of the vertical plate or its length  $L_p$  equal to  $4D$  in the case where the plate is placed horizontally.

## References

- Abbasi, W. S., Saha, S. C., Gu, Y. T., & Ying, Z. C. (2014). Effect of Reynolds numbers on flow past four square cylinders in an in-line square configuration for different gap spacings. *Journal of Mechanical Science and Technology*, 28(2), 539-552. doi: [10.1007/s12206-013-1121-8](https://doi.org/10.1007/s12206-013-1121-8)
- Aboueian, J., & Sohankar, A. (2017). Identification of flow regimes around two staggered square cylinders by a numerical study. *Theoretical and Computational Fluid Dynamics*, 31(3), 295-315. doi: [10.1007/s00162-017-0424-2](https://doi.org/10.1007/s00162-017-0424-2)
- Adeeb, E., Haider, B. A., & Sohn, C. H. (2018). Flow interference of two side-by-side square cylinders using IB-LBM—Effect of corner radius. *Results in Physics*, 10, 256-263. doi: [10.1016/j.rinp.2018.05.039](https://doi.org/10.1016/j.rinp.2018.05.039)
- Admi, Y., Lahmer, E. B., Moussaoui, M. A., & Mezrhab, A. (2021). Numerical study of the drag force reduction and heat transfer characteristics around a heated square cylinder by using three numerical study of the drag force reduction and heat transfer characteristics around a heated square cylinder. *Science International*, 33(5), 385-389. doi: [10.5281/zenodo.5522390](https://doi.org/10.5281/zenodo.5522390)
- Admi, Y., Lahmer, E. B., Moussaoui, M. A., & Mezrhab, A. (2022). Effect of a Flat Plate on Drag Force Reduction and Heat Transfer Characteristics Around Three Heated Square Obstacles. *Journal of Physics: Conference Series*, 2178(1), 012027. doi: [10.1088/1742-6596/2178/1/012027](https://doi.org/10.1088/1742-6596/2178/1/012027)
- Admi, Y., Moussaoui, M. A., & Mezrhab, A. (2020). Effect of a flat plate on heat transfer and flow past a three side-by-side square cylinders using double MRT-lattice Boltzmann method. In *2nd International Conference on Electronics, Control, Optimization and Computer Science (ICECOCS)* (pp. 1-5). IEEE. doi: [10.1109/ICECOCS50124.2020.9314506](https://doi.org/10.1109/ICECOCS50124.2020.9314506)
- Admi, Y., Moussaoui, M. A., & Mezrhab, A. (2021). Effect of Control Partitions on Drag Reduction and Suppression of Vortex Shedding Around a Bluff Body Cylinder. In *International Conference on Advanced Technologies for Humanity* (pp. 453-463). Springer. Cham. doi: [10.1007/978-3-030-94188-8\\_40](https://doi.org/10.1007/978-3-030-94188-8_40)
- Admi, Y., Moussaoui, M. A., Mezrhab, A., Bottom, V., & Henry, D. Convective heat transfer past a three side-by-side square cylinders using double MRT-lattice Boltzmann method. [sciencesconf.org/cfm2019:244841](https://sciencesconf.org/cfm2019:244841)
- Ali, M. S. M., Doolan, C. J., & Wheatley, V. (2012). Low Reynolds number flow over a square cylinder with a detached flat plate. *International Journal of Heat and Fluid Flow*, 36, 133-141. doi: [10.1016/j.ijheatfluidflow.2012.03.011](https://doi.org/10.1016/j.ijheatfluidflow.2012.03.011)
- Benhamou, J., Admi, Y., Jami, M., Moussaoui, M. A., & Mezrhab, A. (2022, March). 3D Simulation of Natural Convection in a Cubic Cavity with Several Differentially Heated Walls. In *2022 2nd International Conference on Innovative Research in Applied Science, Engineering and Technology (IRASET)* (pp. 1-7). IEEE. doi: [10.1109/iraset52964.2022.9738080](https://doi.org/10.1109/iraset52964.2022.9738080)
- Benhamou, J., Jami, M., Mezrhab, A., Botton, V., & Henry, D. (2020). Numerical study of natural convection and acoustic waves using the lattice Boltzmann method. *Heat Transfer*, 49(6), 3779-3796. doi: [10.1002/htj.21800](https://doi.org/10.1002/htj.21800)
- Bhatnagar, P. L., Gross, E. P., & Krook, M. (1954). A model for collision processes in gases. I. Small amplitude processes in charged and neutral one-component systems. *Physical review*, 94(3), 511. doi: [10.1103/PhysRev.94.511](https://doi.org/10.1103/PhysRev.94.511)
- Bouzidi, M. H., Firdaouss, M., & Lallemand, P. (2001). Momentum transfer of a Boltzmann-lattice fluid with boundaries. *Physics of fluids*, 13(11), 3452-3459. doi: [10.1063/1.1399290](https://doi.org/10.1063/1.1399290)
- Breuer, M., Bernsdorf, J., Zeiser, T., & Durst, F. (2000). Accurate computations of the laminar flow past a square cylinder based on two different methods: lattice-Boltzmann and finite-volume. *International journal of heat and fluid flow*, 21(2), 186-196. doi: [10.1016/S0142-727X\(99\)00081-8](https://doi.org/10.1016/S0142-727X(99)00081-8)
- Chatterjee, D., & Mondal, B. (2012). Forced convection heat transfer from tandem square cylinders for various spacing ratios. *Numerical Heat Transfer, Part A: Applications*, 61(5), 381-400. doi: [10.1080/10407782.2012.647985](https://doi.org/10.1080/10407782.2012.647985)
- Chatterjee, D., & Mondal, B. (2013). Mixed convection heat transfer from tandem square cylinders for various gap to size ratios. *Numerical Heat Transfer, Part A: Applications*, 63(2), 101-119. doi: [10.1080/10407782.2012.725007](https://doi.org/10.1080/10407782.2012.725007)
- Dash, S. M., Triantafyllou, M. S., & Alvarado, P. V. Y. (2020). A numerical study on the enhanced drag reduction and wake regime control of a square cylinder using dual splitter plates. *Computers & Fluids*, 199, 104421. doi: [10.1016/j.compfluid.2019.104421](https://doi.org/10.1016/j.compfluid.2019.104421)
- Dey, P. (2022). Fluid flow and heat transfer around square cylinder with dual splitter plates arranged at novel positions. *Proceedings of the Institution of Mechanical Engineers, Part C: Journal of Mechanical Engineering Science*, 236(9), 5060-5077. doi: [10.1177/09544062211057832](https://doi.org/10.1177/09544062211057832)
- Dhiman, A. K., Chhabra, R. P., & Eswaran, V. (2005). Flow and heat transfer across a confined square cylinder in the steady flow regime: effect of Peclet number. *International Journal of Heat and Mass Transfer*, 48(21-22), 4598-4614. doi: [10.1016/j.ijheatmasstransfer.2005.04.033](https://doi.org/10.1016/j.ijheatmasstransfer.2005.04.033)
- d'Humières, D. (2002). Multiple-relaxation-time lattice Boltzmann models in three dimensions. *Philosophical Transactions of the Royal Society of London. Series A: Mathematical, Physical and Engineering Sciences*, 360(1792), 437-451. doi: [10.1098/rsta.2001.0955](https://doi.org/10.1098/rsta.2001.0955)
- Doolan, C. J. (2009). Flat-plate interaction with the near wake of a square cylinder. *AIAA journal*, 47(2), 475-479. doi: [10.2514/1.40503](https://doi.org/10.2514/1.40503)
- Florides, G., & Kalogirou, S. (2007). Ground heat exchangers—A review of systems, models and applications. *Renewable energy*, 32(15), 2461-2478. doi: [10.1016/j.renene.2006.12.014](https://doi.org/10.1016/j.renene.2006.12.014)
- Guo, S., Feng, Y., Jacob, J., Renard, F., & Sagaut, P. (2020). An efficient lattice Boltzmann method for compressible aerodynamics on D3Q19 lattice. *Journal of Computational Physics*, 418, 109570. doi: [10.1016/j.jcp.2020.109570](https://doi.org/10.1016/j.jcp.2020.109570)

- Han, Z., Zhou, D., & Tu, J. (2013). Laminar flow patterns around three side-by-side arranged circular cylinders using semi-implicit three-step Taylor-characteristic-based-split (3-TCBS) algorithm. *Engineering Applications of Computational Fluid Mechanics*, 7(1), 1-12. doi: [10.1080/19942060.2013.11015450](https://doi.org/10.1080/19942060.2013.11015450)
- Harte, R., & Van Zijl, G. P. (2007). Structural stability of concrete wind turbines and solar chimney towers exposed to dynamic wind action. *Journal of Wind engineering and industrial aerodynamics*, 95(9-11), 1079-1096. doi: [10.1016/j.jweia.2007.01.028](https://doi.org/10.1016/j.jweia.2007.01.028)
- Islam, S. U., Abbasi, W. S., & Ying, Z. C. (2016). Transitions in the unsteady wakes and aerodynamic characteristics of the flow past three square cylinders aligned inline. *Aerospace science and technology*, 50, 96-111. Doi: [10.1016/j.ast.2015.12.004](https://doi.org/10.1016/j.ast.2015.12.004)
- Islam, S. U., Rahman, H., Abbasi, W. S., & Shahina, T. (2015). Lattice Boltzmann study of wake structure and force statistics for various gap spacings between a square cylinder with a detached flat plate. *Arabian Journal for Science and Engineering*, 40(8), 2169-2182. doi: [10.1007/s13369-015-1648-3](https://doi.org/10.1007/s13369-015-1648-3)
- Koutmos, P., Papailiou, D., & Bakroziis, A. (2004). Experimental and computational study of square cylinder wakes with two-dimensional injection into the base flow region. *European Journal of Mechanics-B/Fluids*, 23(2), 353-365. doi: [10.1016/j.euromechflu.2003.09.004](https://doi.org/10.1016/j.euromechflu.2003.09.004)
- Kumar, A., Dhiman, A., & Baranyi, L. (2015). CFD analysis of power-law fluid flow and heat transfer around a confined semi-circular cylinder. *International Journal of Heat and Mass Transfer*, 82, 159-169. doi: [10.1016/j.ijheatmasstransfer.2014.11.046](https://doi.org/10.1016/j.ijheatmasstransfer.2014.11.046)
- Kumar, D., & Sen, S. (2021). Flow-induced vibrations of a pair of in-line square cylinders. *Physics of Fluids*, 33(4), 043602. doi: [10.1063/5.0038714](https://doi.org/10.1063/5.0038714)
- Lahmer, E. B., Admi, Y., Moussaoui, M. A., & Mezhhab, A. (2022). Improvement of the heat transfer quality by air cooling of three-heated obstacles in a horizontal channel using the lattice Boltzmann method. *Heat Transfer*, 1-23; doi: [10.1002/htj.22481](https://doi.org/10.1002/htj.22481)
- Lahmer, E. B., Benhamou, J., Admi, Y., Moussaoui, M. A., Jami, M., Mezhhab, A., & Phanden, R. K. (2022). Assessment of conjugate and convective heat transfer performance over a partitioned channel within backward-facing step using the lattice boltzmann method. *Journal of Enhanced Heat Transfer*, 29(3). doi: [10.1615/JEnhHeatTransf.2022040357](https://doi.org/10.1615/JEnhHeatTransf.2022040357)
- Lahmer, E. B., Moussaoui, M. A., & Mezhhab, A. (2019). Investigation of laminar flow and convective heat transfer in a constricted channel based on double MRT-LBM. In *2019 International Conference on Wireless Technologies, Embedded and Intelligent Systems (WITS)* (pp. 1-6). IEEE. doi: [10.1109/WITS.2019.8723820](https://doi.org/10.1109/WITS.2019.8723820)
- Lallemand, P., & Luo, L. S. (2000). Theory of the lattice Boltzmann method: Dispersion, dissipation, isotropy, Galilean invariance, and stability. *Physical review E*, 61(6), 6546. doi: [10.1103/PhysRevE.61.6546](https://doi.org/10.1103/PhysRevE.61.6546)
- Malekzadeh, S., & Sohankar, A. (2012). Reduction of fluid forces and heat transfer on a square cylinder in a laminar flow regime using a control plate. *International Journal of Heat and Fluid Flow*, 34, 15-27. doi: [10.1016/j.ijheatfluidflow.2011.12.008](https://doi.org/10.1016/j.ijheatfluidflow.2011.12.008)
- Manzoor, R., Khalid, A., Khan, I., Baleanu, D., & Nisar, K. S. (2020). Numerical simulation of drag reduction on a square rod detached with two control rods at various gap spacing via lattice Boltzmann method. *Symmetry*, 12(3), 475. doi: [10.3390/SYM12030475](https://doi.org/10.3390/SYM12030475)
- McNamara, G. R., & Zanetti, G. (1988). Use of the Boltzmann equation to simulate lattice-gas automata. *Physical review letters*, 61(20), 2332. doi: [10.1103/PhysRevLett.61.2332](https://doi.org/10.1103/PhysRevLett.61.2332)
- Mezhhab, A., Moussaoui, M. A., Jami, M., Naji, H., & Bouzidi, M. H. (2010). Double MRT thermal lattice Boltzmann method for simulating convective flows. *Physics Letters A*, 374(34), 3499-3507. <https://doi.org/10.1016/j.physleta.2010.06.059>
- Mezhhab, A., Moussaoui, M. A., Jami, M., Naji, H., & Bouzidi, M. H. (2010). Double MRT thermal lattice Boltzmann method for simulating convective flows. *Physics Letters A*, 374(34), 3499-3507. doi: [10.1016/j.physleta.2010.06.059](https://doi.org/10.1016/j.physleta.2010.06.059)
- Mohamad, A. A. (2011). Lattice Boltzmann Method (Vol. 70). London: Springer. Doi: [10.1007/978-1-4471-7423-3](https://doi.org/10.1007/978-1-4471-7423-3)
- Monat, J. P., & Gannon, T. F. (2018). Applying systems thinking to engineering and design. *Systems*, 6(3), 34. doi: [10.3390/systems6030034](https://doi.org/10.3390/systems6030034)
- Moussaoui, M. A., Admi, Y., Lahmer, E. B., & Mezhhab, A. (2021). Numerical investigation of convective heat transfer in fluid flow past a tandem of triangular and square cylinders in channel. *IOP Conference Series: Materials Science and Engineering*. doi: [10.1088/1757-899x/1091/1/012058](https://doi.org/10.1088/1757-899x/1091/1/012058)
- Moussaoui, M. A., Jami, M., Mezhhab, A., & Naji, H. (2009). Convective heat transfer over two blocks arbitrary located in a 2D plane channel using a hybrid lattice Boltzmann-finite difference method. *Heat and mass transfer*, 45(11), 1373-1381. doi: [10.1007/s00231-009-0514-9](https://doi.org/10.1007/s00231-009-0514-9)
- Moussaoui, M. A., Jami, M., Mezhhab, A., & Naji, H. (2010). MRT-Lattice Boltzmann simulation of forced convection in a plane channel with an inclined square cylinder. *International Journal of Thermal Sciences*, 49(1), 131-142. doi: [10.1016/j.ijthermalsci.2009.06.009](https://doi.org/10.1016/j.ijthermalsci.2009.06.009)
- Moussaoui, M. A., Jami, M., Mezhhab, A., Naji, H., & Bouzidi, M. (2010). Multiple-relaxation-time lattice Boltzmann computation of channel flow past a square cylinder with an upstream control bi-partition. *International journal for numerical methods in fluids*, 64(6), 591-608. doi: [10.1002/fld.2159](https://doi.org/10.1002/fld.2159)
- Moussaoui, M. A., Lahmer, E. B., Admi, Y., & Mezhhab, A. (2019, April). Natural convection heat transfer in a square enclosure with an inside hot block. In *2019 International Conference on Wireless Technologies, Embedded and Intelligent Systems (WITS)* (pp. 1-6). IEEE. doi: [10.1109/WITS.2019.8723863](https://doi.org/10.1109/WITS.2019.8723863)
- Moussaoui, M. A., Mezhhab, A., & Naji, H. (2011). A computation of flow and heat transfer past three heated cylinders in a vee shape by a double distribution MRT thermal lattice Boltzmann model. *International journal of thermal sciences*, 50(8), 1532-1542. doi: [10.1016/j.ijthermalsci.2011.03.011](https://doi.org/10.1016/j.ijthermalsci.2011.03.011)
- Nazeer, G., Shams-ul-Islam, Shigri, S. H., & Saeed, S. (2019). Numerical investigation of different flow regimes for multiple staggered rows. *AIP Advances*, 9(3), 035247. doi: [10.1063/1.5091668](https://doi.org/10.1063/1.5091668)
- Nguyen, V. L., Nguyen-Thoi, T., & Duong, V. D. (2021). Characteristics of the flow around four cylinders of various shapes. *Ocean Engineering*, 238, 109690. doi: [10.1016/j.oceaneng.2021.109690](https://doi.org/10.1016/j.oceaneng.2021.109690)
- Rabiee, A. H., Barzan, M. R., & Mohammadebrahim, A. (2021). Flow-induced vibration suppression of elastic square cylinder using windward-suction-leeward-blowing approach. *Applied Ocean Research*, 109, 102552. doi: [10.1016/j.apor.2021.102552](https://doi.org/10.1016/j.apor.2021.102552)
- Rahim, K. Z., Ahmed, J., Nag, P., & Molla, M. M. (2020). Lattice Boltzmann simulation of natural convection and heat transfer from multiple heated blocks. *Heat Transfer*, 49(4), 1877-1894. doi: [10.1002/htj.21698](https://doi.org/10.1002/htj.21698)
- Rashidi, S., Dehghan, M., Ellahi, R., Riaz, M., & Jamal-Abad, M. T. (2015). Study of stream wise transverse magnetic fluid flow with heat transfer around an obstacle embedded in a porous medium. *Journal of Magnetism and Magnetic Materials*, 378, 128-137. doi: [10.1016/j.jmmm.2014.11.020](https://doi.org/10.1016/j.jmmm.2014.11.020)
- Rashidi, S., Hayatdavoodi, M., & Esfahani, J. A. (2016). Vortex shedding suppression and wake control: A review. *Ocean Engineering*, 126, 57-80. doi: [10.1016/j.oceaneng.2016.08.031](https://doi.org/10.1016/j.oceaneng.2016.08.031)
- Shamsoddini, R., Sefid, M., & Fatehi, R. (2014). ISPH modelling and analysis of fluid mixing in a microchannel with an oscillating or a rotating stirrer. *Engineering Applications of Computational Fluid Mechanics*, 8(2), 289-298. doi: [10.1080/19942060.2014.11015514](https://doi.org/10.1080/19942060.2014.11015514)
- Sohankar, A., & Najafi, M. (2018). Control of vortex shedding, forces and heat transfer from a square cylinder at incidence

- by suction and blowing. *International Journal of Thermal Sciences*, 129, 266-279. doi: [10.1016/j.ijthermalsci.2018.03.014](https://doi.org/10.1016/j.ijthermalsci.2018.03.014)
- Sumner, D. (2010). Two circular cylinders in cross-flow: a review. *Journal of fluids and structures*, 26(6), 849-899. doi: [10.1016/j.jfluidstructs.2010.07.001](https://doi.org/10.1016/j.jfluidstructs.2010.07.001)
- Tamimi, V., Naeeni, S. T. O., & Zeinoddini, M. (2017). Flow induced vibrations of a sharp edge square cylinder in the wake of a circular cylinder. *Applied Ocean Research*, 66, 117-130. doi: [10.1016/j.apor.2017.05.011](https://doi.org/10.1016/j.apor.2017.05.011)
- Tong, F., Cheng, L., Zhao, M., & An, H. (2015). Oscillatory flow regimes around four cylinders in a square arrangement under small and conditions. *Journal of Fluid Mechanics*, 769, 298-336. doi: [10.1017/jfm.2015.107](https://doi.org/10.1017/jfm.2015.107)
- Turki, S. (2008). Numerical simulation of passive control on vortex shedding behind square cylinder using splitter plate. *Engineering Applications of Computational Fluid Mechanics*, 2(4), 514-524. doi: [10.1080/19942060.2008.11015248](https://doi.org/10.1080/19942060.2008.11015248)
- Vamsee, G. R., De Tena, M. L., & Tiwari, S. (2014). Effect of arrangement of inline splitter plate on flow past square cylinder. *Progress in Computational Fluid Dynamics, an International Journal*, 14(5), 277-294. doi: [10.1504/PCFD.2014.064554](https://doi.org/10.1504/PCFD.2014.064554)
- Wu, H. W., Perng, S. W., Huang, S. Y., & Jue, T. C. (2006). Transient mixed convective heat transfer predictions around three heated cylinders in a horizontal channel. *International Journal of Numerical Methods for Heat & Fluid Flow*, 16(6), 674-692; doi: [10.1108/09615530610679057](https://doi.org/10.1108/09615530610679057)
- Yang, Z., Ding, L., Zhang, L., Yang, L., & He, H. (2020). Two degrees of freedom flow-induced vibration and heat transfer of an isothermal cylinder. *International Journal of Heat and Mass Transfer*, 154, 119766. doi: [10.1016/j.ijheatmasstransfer.2020.119766](https://doi.org/10.1016/j.ijheatmasstransfer.2020.119766)
- Zhou, L., Cheng, M., & Hung, K. C. (2005). Suppression of fluid force on a square cylinder by flow control. *Journal of Fluids and Structures*, 21(2), 151-167. doi: [10.1016/j.jfluidstructs.2005.07.002](https://doi.org/10.1016/j.jfluidstructs.2005.07.002)
- Zou, Q., & He, X. (1997). On pressure and velocity boundary conditions for the lattice Boltzmann BGK model. *Physics of fluids*, 9(6), 1591-1598. doi: [10.1063/1.869307](https://doi.org/10.1063/1.869307)



© 2022. The Author(s). This article is an open access article distributed under the terms and conditions of the Creative Commons Attribution-ShareAlike 4.0 (CC BY-SA) International License (<http://creativecommons.org/licenses/by-sa/4.0/>)